A Home Ignition Assessment Model Applied to Structures in the Wildland-Urban Interface

Kaushik Biswas, PhD
Associate Member ASHRAE

David Werth

Narendra Gupta, PhD

ABSTRACT

The issue of exterior fire threat to buildings, from either wildfires in the wildland-urban interface or neighboring structure fires, is critically important. To address this, the Wildfire Ignition Resistant Home Design (WIRHD) program was initiated. The WIRHD program developed a tool, the WildFIRE Wizard, that will allow homeowners to estimate the external fire threat to their homes based on specific features and characteristics of the homes and yards. The software then makes recommendations to reduce the threat. The inputs include the structural and material features of the home and information about any ignition sources or flammable objects in its immediate vicinity, known as the "home ignition zone."

The tool comprises an ignition assessment model that performs explicit calculations of the radiant and convective heating of the building envelope from the potential ignition sources. This article describes a series of material ignition and flammability tests that were performed to calibrate and/or validate the ignition assessment model. The tests involved exposing test walls with different external siding types to radiant heating and/or direct flame contact. The responses of the test walls were used to determine the conditions leading to melting, ignition, or any other mode of failure of the walls. Temperature data were used to verify the model predictions of temperature rises and ignition times of the test walls.

INTRODUCTION

The wildland-urban interface (WUI) fire problem has appropriately received much attention in the last decade, both in the United States and internationally. The National Interagency Fire Center (NIFC) and the National Fire Protection Association (NFPA) provide a historical perspective on wildland fires in the U.S. in terms of economic loss, loss of life, and the fire size in acres burned (NIFC 2012; NFPA 2012). According to NFPA (2012), the ten largest wildland fires in the U.S. resulted in losses ranging from $396 million to $2.4 billion (adjusted to 2010 dollars). Approximately one hundred lives were lost to wildfire in Europe in 2007 (Lampin-Maillet et al. 2009). In Australia, the 2009 bushfires, among the worst in recent memory, resulted in widespread destruction and significant loss of life. The expanding residential development at the WUI has been widely recognized as a factor influencing forest management policies in the U.S. (Theobold and Romme 2007) and also places property and human life at risk from wildfire destruction (Reams et al. 2005). In 2000, the WUI encompassed 11% of the land area (719,156 km^2) and 38% of all housing units (44.3 million) in the contiguous U.S. (Hammer et al. 2009). Using different metrics, Theobald and Romme (2007) estimated the WUI area to be 465,614 km^2 and projected at least a 10% increase by 2030. Albini (1997) noted in an invited talk to the International Association of Fire Safety Science (IAFSS) that "Interest by the general public in matters of wildland fire safety has grown with increased exposure of affluent society to the hazards posed by building flammable structures in flammable wildland settings."

Recently, Mell et al. (2010) reviewed and summarized the challenges posed by wildfire spreading into the WUI and identified the research needs for addressing the fire problem in terms of laboratory and field experiments and fire behavior models. The article reported that "there is currently no stan-

Kaushik Biswas *is an R&D associate (building scientist) in the Energy and Transportation Science Division at Oak Ridge National Laboratory, Oak Ridge, TN.* ***David Werth*** *is a principal scientist at and* ***Narendra Gupta*** *is retired from Savannah River National Laboratory, Aiken, SC.*

dardized method of risk assessment that can be applied to WUI communities in the US" (p. 240). The research needs identified by Mell et al. include: (1) structure exposure conditions (flame heat flux and firebrands) for a range of WUI settings (terrain, housing density, fuels, etc.), and (2) the vulnerability of a structure or building when subjected to a given exposure. The ignition threat of firebrands and their generation from burning vegetation in wildland fires has also received significant attention (Manzello et al. 2006, 2007, 2009).

There has also been significant work in modeling wildfires and their impacts in the WUI. Papadopoulos and Pavlidou (2011) reviewed various physical, quasi-physical, empirical, and quasi-empirical wildfire models and tabulated their relative merits and disadvantages. Mell et al. (2007) reported the development of a three-dimensional, fully transient, physics-based fire spread model to simulate grassland fires. The authors noted various fire behavior problems that are outside the scope of empirical and semi-empirical models and are only amenable to physical modeling. However, they also recognized the significantly higher computational resources required by the physical models. Rehm (2008) noted that application of physical or field models to compute multiple burning houses and vegetative (WUI) fires over large areas is difficult due to the range of time and spatial scales that need to be solved; time scales associated with this problem range from tens of seconds with burning grass and individual trees to hours for burning structures. The use of field models for modeling large-area WUI fires in the near term is unlikely due to the constraints on the computational resources (Rehm 2008). The key advantages of empirical models, which are based on observation and experiments, are relatively straightforward implementation and direct relation to behavior of real fires (Papadopoulos and Pavlidou 2011). Quasi-empirical models contain statistical analyses based on functional relationships between dependent and independent variables and have the added benefit of reduced influence of the data set size and personal choice (Papadopoulos and Pavlidou 2011).

In 2009, the United States Department of Homeland Security initiated the Wildfire Ignition Resistant Home Design (WIRHD) program to develop a semi-empirical software tool, the Wildfire Ignition Resistance Estimator (WildFIRE) Wizard, which evaluates fire threats to homes and provides guidelines for reducing them. The main outcome of this project is an enhanced ignition assessment model based on the structure ignition assessment model (SIAM) of Cohen (2004), which forms the core of the WildFIRE Wizard. This tool allows homeowners to graphically create a reproduction of their home and yard, including burning objects ("threats") within the home ignition zone (HIZ) that can possibly cause an ignition of the structure. It calculates temperatures and a flux-time product (FTP) from both radiative and convective heating by the threats to estimate the ignition potential of the structure based on field studies and known building material properties (Cohen 2004). One of the major challenges facing decision makers while formulating wildfire risk mitigation programs is how to change the behavior of private property owners regarding vegetation management (Reams et al. 2005). A validated WildFIRE Wizard, an easy-to-use tool needing minor computational resources, will be a major step towards overcoming this challenge.

The ignition model (enhanced SIAM) requires empirical data on the thermal and ignition properties of the external siding materials used on homes. Empirical models should be based on well-characterized, science-based, and repeatable experiments (Mell et al. 2010). This has been partially accomplished through field tests (Cohen 2004), but the full range of model calculations needed verification and validation. Therefore, a series of flammability tests of small-scale wall assemblies with different exterior sidings were conducted. These small-scale tests were specifically designed as surrogates for full-scale field testing of wildfires, which are very difficult to perform for a wide range of wildfire-structure configurations. These tests were interpreted in the context of the model—validating the way the model calculated heat flux from flames and ignition predictions or to determine more appropriate response factors. *PATRAN* (MSC 2008) simulations were also performed to get more detailed information about the thermal responses of the wall assemblies. These simulations were also verified against data from the flammability tests. Once validated, the *PATRAN* models were used as verification tools for the SIAM calculations that could not directly be validated by measurements. In the following sections, the flammability tests and the software validation using test data are presented.

EXPERIMENTAL ARRANGEMENT

The enhanced SIAM accounts for both radiant and convective heating as potential igniters of the home, and various siding samples were tested for several scenarios. The radiant tests were intended for validation of the materials' ignition characteristics, while the convective tests were done to validate the way the model converts a flame of prescribed power into a heat flux. Small-scale wall assemblies of 1.2×1.2 m^2 area were built and exposed to either a radiant source or a flame (or both) of prescribed intensities. The walls were constructed using wood studs and contained fiberglass cavity insulation, with a gypsum board "interior" finish. The test wall "exterior" consisted of oriented strand board (OSB) and different external claddings and was exposed to the different heat sources. Four external cladding types were tested: (1) vinyl siding, (2) cedar wood siding, (3) fiber cement board, and (4) exterior fiber cement board with a 2.54 cm extruded polystyrene (XPS) insulation board underneath.

Each test assembly was subjected to each of the following exposures, chosen to simulate various likely scenarios in the wildland-urban interface:

- Short-duration, high-intensity radiation flux: 40–50 kW/m^2 for a short time (60 s), with a pilot flame. This was designed to simulate radiation from short-exposure actively spreading forest fires (Cohen 2004).

- Direct flame contact: 100 kW flame for 60 s; the flame source was a slot burner adjacent to the wall. This exposure represented burning debris and plants next to the house.
- Long-exposure, coupled radiant heating and direct flame contact: a 25 kW/m^2 radiant source and 100 kW flame from the slot burner. This was to simulate both the radiation from a burning neighboring structure and convective heat from the burning debris next to the house. The combined radiation heat and flame exposure was continued until either the exterior cladding ignited or 15 min had elapsed with no ignition.

Thermocouples were installed at regular intervals on the sample face (Figure 1) and were sampled at 10 Hz. Type K 0.127 mm diameter thermocouples were used, with a tolerance limit of 0.75% for the temperature range of 0°C–1250°C. These were arranged along the vertical and horizontal centerlines both on the exterior surface and behind it (above the OSB layer). In the flame contact tests, two floating thermocouple arrays were also installed along the vertical centerline about 3 mm and 10 mm away from the exterior surface (Figure 1). These were installed to measure the flame temperatures adjacent to the sample surface.

The assembly test data were intended to be used in the following manner:

- Validation of the FTP ignition thresholds for wood siding for use by SIAM.
- Air and surface temperatures to validate the SIAM calculations of the convective heat flux and surface temperatures or determine a more appropriate response function.
- Interior OSB temperatures to determine the failure or ignition of internal layers (especially with cement board siding).
- External and internal surface temperatures to validate the *PATRAN* calculations for the fiber cement tests.

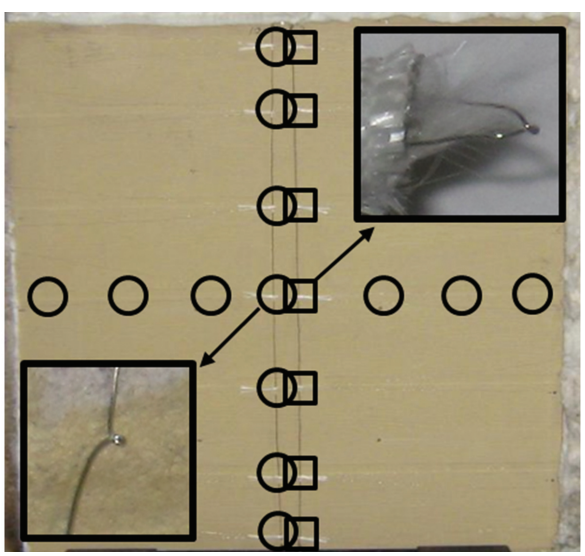

Figure 1 *Test wall sample with surface and floating thermocouples: circles = surface thermocouples; squares = floating thermocouples. Close-up photographs of each type are shown as insets.*

THE STRUCTURE IGNITION ASSESSMENT MODEL (SIAM)

This section describes the essential features of the SIAM. The user inputs details of the home and the HIZ through a graphical user interface. Once the details are obtained, the model operates by first subdividing the walls of the home into a series of panels, each characterized by its height, width, and location, and then defining a series of burning threats that can each impart radiant and convective heat to the different panels. SIAM calculates the heat flux from each threat individually and sums them to get the total heat flux on a panel. For radiation heat flux, the model uses the geometry of the flame front and the wall and their relative positions to calculate the view factor ($V_{f\to w}$) and then the radiation exchange (Q, W) using the following equation for gray, diffuse surfaces (Incropera and Dewitt 1996), using prescribed flame and wall temperatures:

$$Q = \frac{\sigma\left(T_f^4 - T_w^4\right)}{\dfrac{1-\varepsilon_f}{\varepsilon_f A_f} + \dfrac{1}{V_{f\to w} A_f} + \dfrac{1-\varepsilon_w}{\varepsilon_w A_w}} \tag{1}$$

where σ is the Stefan-Boltzmann constant (5.67×10^{-8} W/m$^2\cdot$K^4), T is the temperature, ε is the emissivity, and A is the projected area; subscripts f and w represent the flame and wall, respectively. Equation 1 is specific to a two-surface enclosure, in which the two surfaces only exchange radiation with each other, and is not an accurate representation of a fire threat facing a wall. However, this represents the worst-case scenario since all the radiant heat of the flame is assumed to be impinging on the wall. Radiation heat fluxes on the wall were calculated using the two-surface enclosure scenario, a three-surface enclosure formulation with the environment as the third surface (Modest 1993), net radiation exchange at the wall surface formulation (Modest 1993) and the original SIAM radiation heat transfer equation (Cohen 2004). The two-surface enclosure equation (Equation 1) yielded the highest heat flux impinging on the wall.

For convective heating, the model uses the wall height and flame position and length to calculate the point on the wall at which the flame or the hot air column above the flame intercepts the wall. Given the temperature difference, a modified heat transfer equation calculates the convective heat flux.

The heat fluxes produced by these calculations serve as input to two other algorithms that determine the response of

the home, which depends on the siding. Vinyl absorbs heat until the melting point is reached, following which it is assumed that the siding falls away from the wall, exposing the interior layers. Wood siding absorbs heat until it ignites, and this is done according to an empirical equation (Cohen 2004). Both these calculation procedures were calibrated or validated with the current flammability tests and are described in the Test Results and Discussion section. In the tests for this research, the radiation heat flux was prescribed and, therefore, the radiation flux calculation procedure was not used for the simulations. The primary intent for the purposes of this paper was to collect data from the sample tests and apply them to the model algorithms to determine if the model can accurately reproduce the responses of the test samples.

TEST RESULTS AND DISCUSSION

Radiant Heating

The radiant heating tests involved the use of a calibrated radiant panel, shown in Figure 2, which could be adjusted to impart any desired heat flux to the samples. The radiant panel consisted of a thick metal sheet heated by gas-fired burners, and the desired heat flux was obtained by adjusting the fuel flow rate to the burners and the distance between the radiant panel and the test walls. The radiant heat flux incident on the test samples was calibrated using a panel instrumented with five radiometers (Figure 2). Heat flux calibration tests were performed both before and after the samples were tested at each desired radiant exposure (25, 40, and 50 kW/m^2). Figure 3 shows the pre- and post-test calibration plots for the 40 kW/m^2 radiant flux, which showed little loss of calibration between measurements.

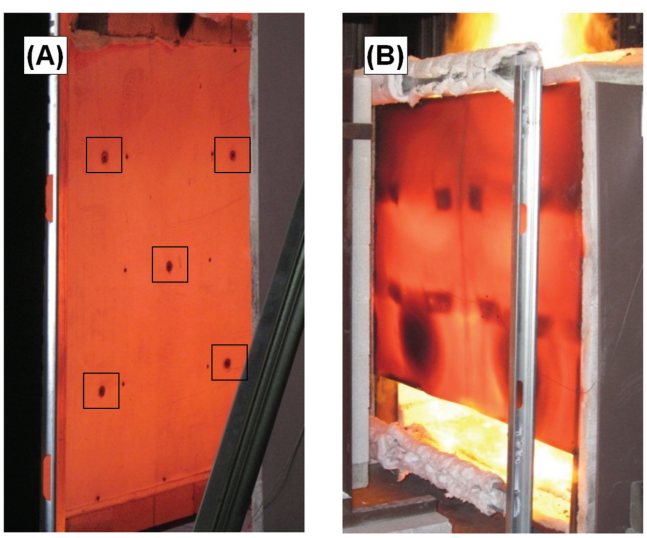

Figure 2 *(A) Calibration panel instrumented with five radiometers (indicated by □) and (B) radiant panel heated by gas-fired burners.*

For this first set of tests, the 40 and 50 kW/m^2 exposures were used, and the test walls were exposed to the radiant panel after a 15 min warm-up period. The heat flux values used as inputs to the model calculations are based on the calibration panel tests. These tests were used to validate the simulated response of the samples. Data from two radiant tests are presented: a vinyl sample and a cedar siding sample, each of which is treated differently in SIAM.

Vinyl Sample. Figure 4 shows the instrumentation of the vinyl wall sample for the radiant exposure test. Thermocouples were installed along the vertical and horizontal centerlines on the exterior vinyl and interior OSB surfaces. This test involved the application of the calibrated 40 kW/m^2 radiant heat flux to the wall sample with vinyl siding. SIAM uses an explicit heat transfer equation to calculate the vinyl temperature T, removing the siding to expose the OSB underneath when the melting temperature is exceeded. This is done according to Equation 2:

$$T_{t+1} = T_t + \left(\frac{Q'' - C}{C_p}\right) \Delta t, \text{ for } Q'' > C \qquad (2)$$

where Q'' is the imposed heat flux (kW/m^2), heat capacity C_p = 1287 J/m^2·K for vinyl, Δt is the time step, and C is a prescribed cooling rate (in kW/m^2) to account for the heat loss to the surroundings. The heat capacity was based on the

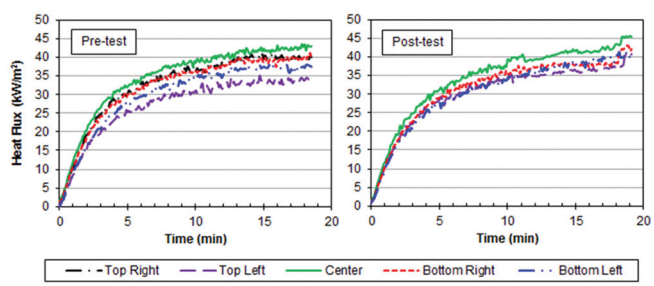

(A) (B)

Figure 3 *(A) pre-test and (B) post-test radiant panel calibration data for the 40 kW/m^2 heat flux.*

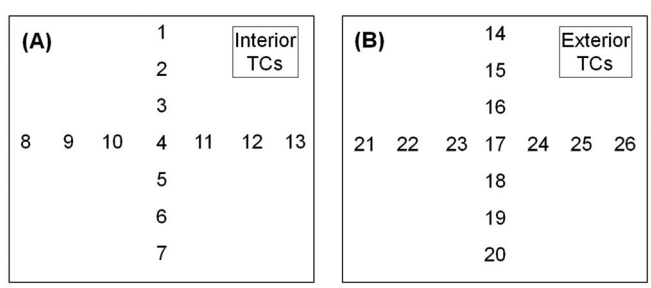

Figure 4 *Interior and exterior thermocouple (TC) locations for the vinyl radiant exposure test sample.*

measured specific heat (c_p) of vinyl according to ASTM E 1269 (2011a). The imposed heat flux (Q'') was 38.44 kW/m^2, which was the average heat flux measured from 15:00 to 15:30 min in the 40 kW/m^2 calibration tests. The cooling rate (C) represents a reduction in the rate at which the vinyl temperature increases; it was estimated according to the rate at which the actual vinyl sample heated up.

Measured interior and exterior vinyl surface temperatures were averaged to get the vinyl temperature and compared to calculated temperatures, as shown in Figure 5. The sample temperatures showed an approximately linear increase with time in response to the constant heating rate, at an average of 5.19°C/s. Different cooling rates were tested in the SIAM calculations and 31.8 kW/m^2 was chosen as the optimum cooling rate, which yielded a temperature rise rate of 5.16°C/s. Equation 2 in the ignition model was therefore recoded with the updated cooling rate, and the model was modified so that the vinyl siding temperature rise occurs only when the imposed heat flux exceeds 31.8 kW/m^2.

This test was also useful for determining the melting point of the vinyl siding, which the model uses to determine when the siding has ablated and exposed the interior OSB. The interior thermocouples (Figure 6) showed a sharp rise in temperature when the siding failed, which occurred when the exterior vinyl temperature was between 230°C and 310°C. An average value of 270°C was assigned in the SIAM module for vinyl siding melting.

Cedar Sample. This test also used a 40 kW/m^2 radiant heat panel but applied it to a cedar siding wall, which was also instrumented as shown in Figure 4. For wood siding, the model uses the FTP calculation of Cohen (2004) to establish ignition. The radiant heating is used to calculate the FTP value according to Equation 3:

$$FTP = \int (Q'' - Q''_C)^{1.828}\, dt, \text{ for } Q'' > Q''_C \qquad (3)$$

where Q''_C is the critical radiant heat flux (13.1 kW/m^2) (Cohen 2004) and Q'' = 38.44 kW/m^2 from the calibration panel tests. As the FTP values crosses 11500, ignition is more and more likely until the value of 13500 is reached, when it is a certainty (Cohen 2004). The FTP value increases until the heating stops or the ignition threshold is reached. The goal of this test was to determine if the threshold value obtained by earlier research (Cohen 2004) is accurate enough to be used in the model. With Q'' = 38.44 kW/m^2, Equation 3 predicted ignition between 32 and 37 s, going from likely to certain ignition. In the test, ignition, as indicated by the jump in temperature of thermocouples 16–18 (Figure 7), occurred at about 28 s after exposure, close to the value predicted by the model.

This test was rendered less conclusive by the fact that the pilot flame intended to ignite the sample after off-gassing began was extinguished and had to be relit. Off-gassing was observed to start after 10 s, with the siding becoming dark after 19 s. The sample ignited immediately after the pilot light was relit at 27 s, so it was concluded that this test still represents a good confirmation of the ignition threshold currently used by the model.

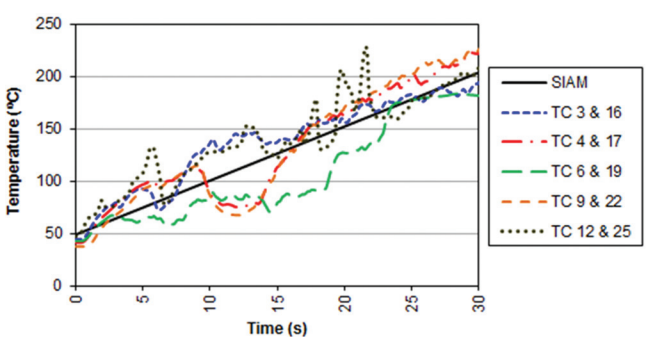

Figure 5 *Measured (TC) and calculated (SIAM) temperatures of vinyl sample during the 40 kW/m^2 radiant exposure test. Measured temperatures are averages of the interior and exterior thermocouples.*

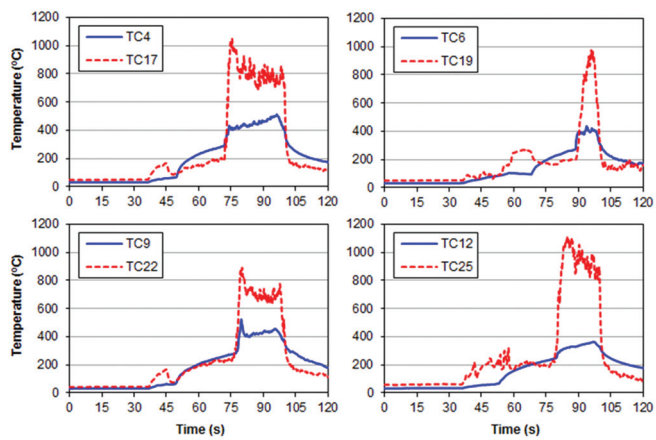

Figure 6 *Measured interior (solid blue) and exterior (dashed red) vinyl siding temperatures for the radiant exposure test.*

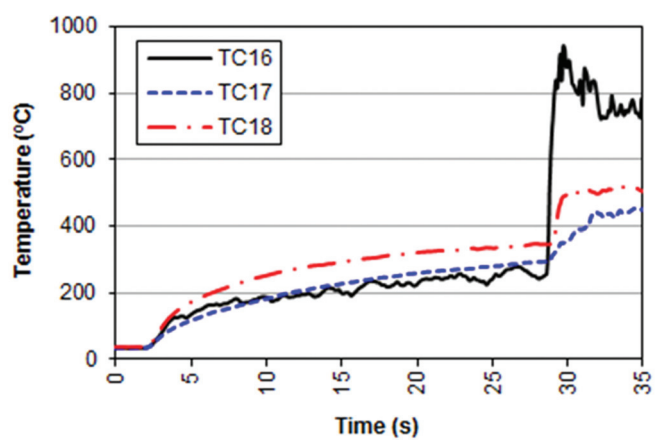

Figure 7 *Measured external cedar siding temperature in response to 40 kW/m^2 radiant heating.*

Convective Heating

Convective heating is imparted to the sample from either active flames or the hot air column above a flame front that is in position to allow for contact. A propane-fueled slot burner of approximately half the width of the test walls was used for the convective heating tests.

Figure 8 shows the slot burner and a test in progress (fiber cement sample). The fuel flow rate was adjusted to get the desired 100 kW flame (based on the lower heating value) output using an air calibrated rotameter. Results from these tests were used to help calibrate this process and provide some further validation of the model adjustments made in response to earlier tests.

Cedar Sample. This test comprises a 100 kW flame applied to a wall with cedar siding. The model calculates the heat flux by calculating a flame/air column temperature (T_f) and assuming a wall temperature (T_w), then applying the following heat transfer equation:

$$Q'' = h(T_f - T_w) \tag{4}$$

Here h is the heat transfer coefficient (kW/m^2·K). The model assumes a flame temperature and a hot air column above the flame tip that is relatively cooler. T_f can represent either the flame or the hot air temperature. For T_w, the model assumes a constant value of 32°C (instead of solving for the wall temperature explicitly) to maintain a conservatively large heat flux. This was necessary as, in order to simplify the process and speed up the calculations, the heat transfer module calculates and saves all heat fluxes during the burning time, which then serve as input to a separate module that calculates the thermal response of the siding. As before, the cedar ignition was estimated by calculating the FTP value. The ignition time in the experiment was 25 s after exposure, so the heat transfer coefficient (h) needed to be calibrated so that the heat flux was such that the FTP reached the critical value at the appropriate time.

Figure 9 shows the locations of the thermocouples on the cedar wall sample. The instrumentation consisted of interior and exterior surface and floating air thermocouples. Ignition was first observed at the lower edge of the sample, so the temperature reading of TC21 was used as the flame temperature. The model originally used an algorithm to determine h at each time step, which produced a series of values ranging between 20 and 40 kW/m^2·K. The simulated heat flux calculated using the above values of h resulted in FTP values that did not reach the critical FTP needed for ignition at the proper time, remaining below the threshold long past the point at which the test sample actually ignited. The model was, therefore, updated by assigning a constant value of 58.42 kW/m^2·K to h.

The heat flux was calculated using the updated value of h in Equation 4 and then the FTP was calculated by Equation 3. Figure 10 shows the evolution of the convective heat flux and resultant FTP with the original and revised val-

Figure 8 *Burner used for convective heating of the test samples.*

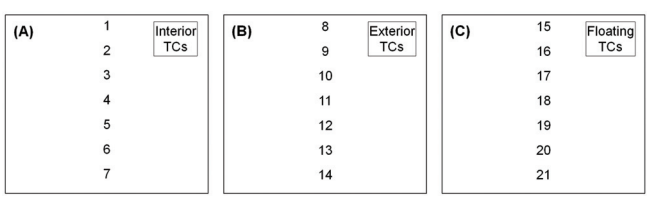

Figure 9 *Thermocouple (TC) locations for the cedar convective exposure test sample.*

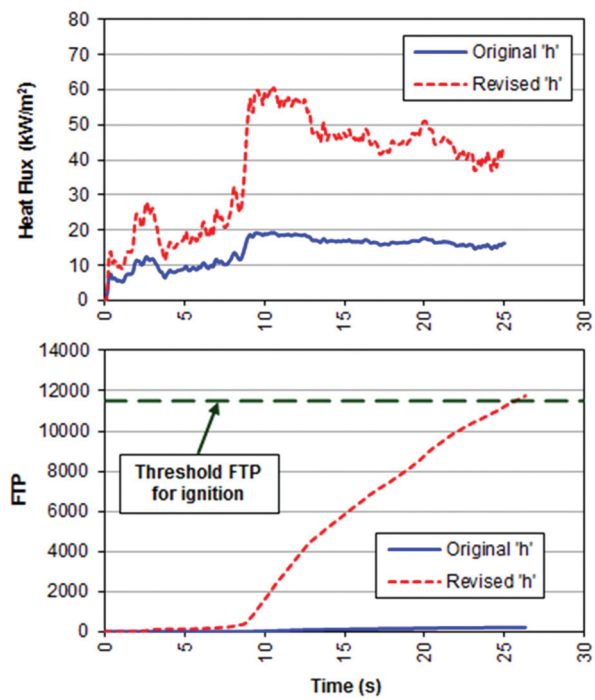

Figure 10 *Heat fluxes calculated with the original and revised* h *values (top) and the corresponding FTP values (bottom) for the cedar sample exposed to*

ues of h. The calculation yielded an FTP curve that reached 11236 at 25 s with an h of 58.42 kW/m^2·K, the same time as the actual ignition. This value was therefore selected as the optimal heat transfer coefficient in the model.

Vinyl Sample. Next, the 100 kW flame was applied to a wall sample with vinyl siding, with the thermocouple locations as shown in Figure 9, except no floating air thermocouples were used. This test was used to validate the parameters derived in previously described tests: (1) the constant value of h (58.42 kW/m^2·K) and (2) the vinyl cooling rate (C) of 31.8 kW/m^2. For this test, since no floating thermocouples were used, TC16 from the cedar flame test (Figure 9) was selected to represent the flame temperature (T_f). The focus here was on the response of the upper half of the sample. The top half was exposed to the hot gases and the fire plume, rather than direct flame, which would have caused immediate melting of the vinyl siding. The flame/hot air temperature was used in Equation 4 to get the heat flux into the sample (assuming a constant T_w = 32°C and h = 58.42 kW/m^2·K).

Next, the calculated convective heat flux was used in Equation 2 to calculate the sample temperature, and this was compared to the measured temperatures, averaged over the inner and outer probes, of the top half of the wall. The comparison of the measured and calculated temperatures is shown in Figure 11. The calculated temperature provides a good approximation of the measured interior and exterior wall temperatures, verifying the revisions to Equations 2 and 4.

Fiber Cement Sample. Many modern homes are covered with fiber cement siding, which is considered fire resistant up to very high temperatures, and the model currently considers such siding to be failure-proof. To validate this, tests were conducted on wall samples with fiber cement siding. These were also simulated with the *PATRAN* radiative transfer software, which provided a more detailed picture of heat transfer within the material. These tests of the software are also valuable because *PATRAN* has been used extensively to verify the SIAM algorithms—so comparing the *PATRAN* calculations with the experimental data from the tests provided the necessary independent check.

The actual wall specimens measured 1.2 × 1.2 m^2, but to reduce the computation time, 0.6 × 0.6 m^2 samples were simulated, with the four edges assigned adiabatic boundary conditions because of symmetry. Scoping results for symmetric radiant heat flux loading conditions showed that the end effects were minimal and two-dimensional models would yield equally good results.

Besides the imposed heat flux, the boundary conditions for the simulated heat flux loading must include convective and radiation losses to the ambient from the wall surface. For the 100 kW flame, it was not possible to estimate the heat losses from the flame to the ambient. Therefore, the temperatures recorded by the thermocouples offset from the wall were used as the flame temperature, and forced convection with 5 m/s flame velocity was used. The velocity was chosen based on measurements and simulations of a buoyant methane fire stabilized on a 1 m diameter fuel source (Tieszen et al. 2002; Xin et al. 2008). The initial temperature of the whole assembly in the *PATRAN* model was 25°C. The fiber cement board wall geometry used for the model is shown in Figure 12.

Fiber cement siding is not expected to ignite, but it may fail if it becomes too hot or allows too much heat to pass through its interior into its supporting material. These tests and the associated *PATRAN* simulations were performed to determine that *PATRAN* can accurately simulate heat transfer through the siding, a key variable in estimating the possibility of failure.

In this test, the fiber cement siding sample was exposed to the 100 kW flame. Figure 13 shows a comparison of the calculated *PATRAN* temperature at the center of the panel with the measurements from thermocouples TC11 and TC12. The thermocouple locations for the fiber cement sample were the same as those for the cedar sample (Figure 9). The calculated temperatures were within 10% of the measurements, except at the beginning of the calculations when the difference

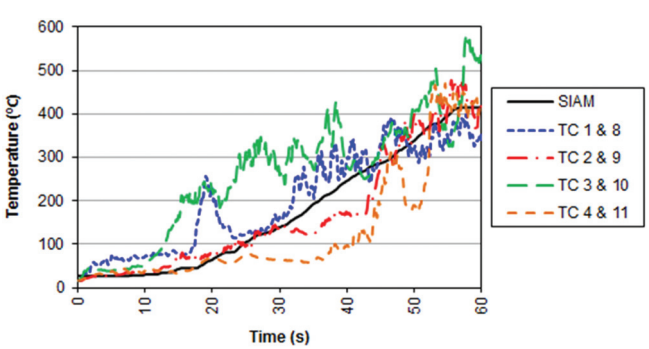

Figure 11 *Measured (TC) and calculated (SIAM) temperatures of the vinyl sample when exposed to a 100 kW flame. Measured temperatures are averages of the interior and exterior thermocouples.*

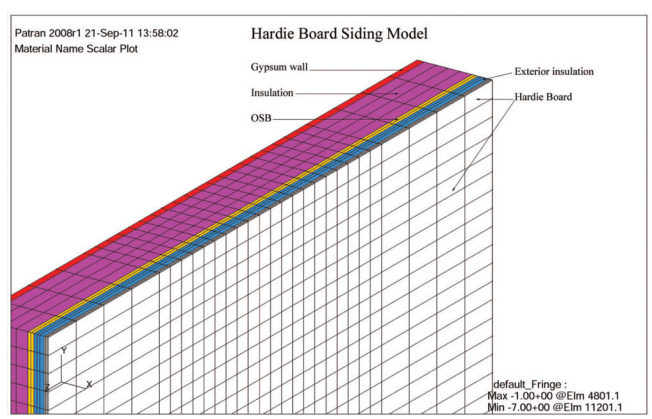

Figure 12 *Fiber cement wall thermal model geometry used in PATRAN simulations.*

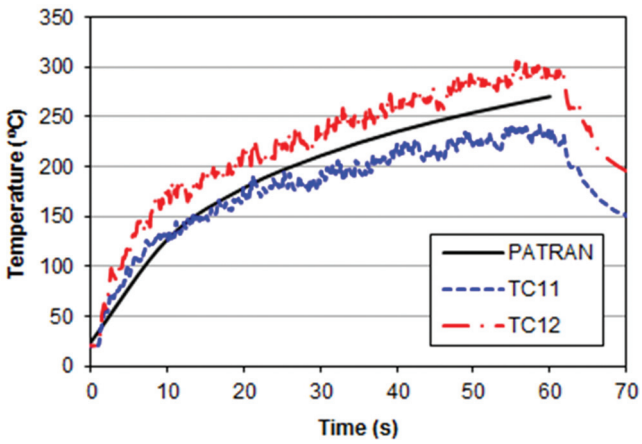

Figure 13 *Measured (TC) and PATRAN calculated surface temperatures of the fiber cement sample exposed to the 100 kW flame.*

was about 20% with the prescribed 25°C initial model temperature.

Fiber cement boards are rated non-combustible up to 750°C, according to ASTM non-combustibility test, ASTM E 136 (2011b). The measured temperatures rose to about 300°C during this short-duration convective heating test and there were no signs of ignition or other visible failure of the wall, other than some surface charring, at the end of the test.

Fiber Cement Sample with XPS Backing. This test also used the 100 kW flame heating, but here the test specimen had the XPS insulation inserted between the fiber cement siding and the OSB. Figure 14 compares the *PATRAN* calculated surface temperatures to the measured internal and external surface temperatures.

The *PATRAN* calculations of this test did not match the test data very well, with up to 50% differences between measurements and calculations. Part of the discrepancy can be attributed to measurement uncertainties. Comparing the external temperatures between this and the previous test (Figure 13), temperature differences of 100°C or more were observed for the same location. However, the test did show that the siding/XPS construction withstood the 100 kW exposure without any ignition or visible failure. It is also quite evident that the XPS temperatures did not rise enough to cause internal failure of the wall. The melting (softening) temperature of XPS is 104°C and its flash point is greater than 324°C.

Combined Radiant and Convective Heating

Cedar Sample. This test involved both a radiant panel (25 kW/m^2) and a flame (100 kW) applied to a cedar siding wall. For this test, the radiant panel was allowed a 7 min warm-up period before the test was initiated. A radiant heat flux of 27.36 kW/m^2, based on the pre- and post-test calibration data, was used for the calculations. Figure 15 shows the arrangement of thermocouples for this test.

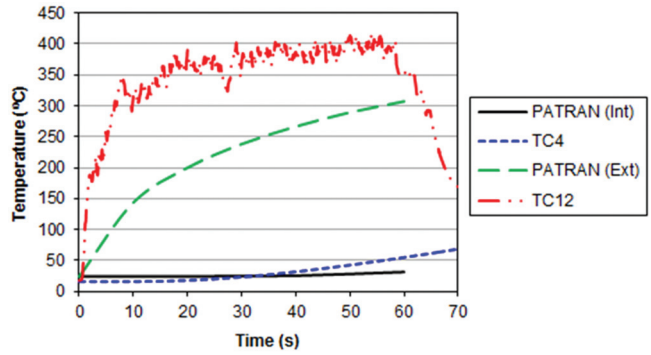

Figure 14 *Measured (TC) and PATRAN calculated surface temperatures of the fiber cement sample exposed to the 100 kW flame; TC4 = internal surface and TC12 = external surface.*

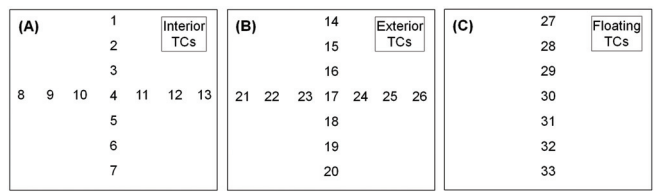

Figure 15 *Thermocouple (TC) locations for the cedar sample for the combined radiant and convective exposure test.*

First, the convective heat flux was calculated using Equation 4, again with the lower-edge floating temperature probe (TC33) as the flame temperature and h = 58.42 kW/m^2·K, based on prior calculations. Next, the constant radiant heat flux was added to get the total heat flux. The total heat flux was entered into the FTP equation (Equation 3) to calculate the ignition time, which was 5.8 s (when the FTP crossed the threshold value of 11,500). Figure 16 shows the calculated heat flux and resulting FTP values. Figure 17 shows the measured external cedar siding temperatures. Unlike the 40 kW/m^2 radiant heating exposure (Figure 7), no sharp temperature rises were observed to indicate wall ignition. Based on video evidence, the cedar sample ignited between 7 to 10 s after exposure. The calculated ignition time of 5.8 s is a close match to the actual ignition time, validating the revised convective heat flux calculation.

Fiber Cement Sample with XPS Backing. In this test, the fiber cement siding/XPS construction was exposed for a full 13 min to the combined 25 kW/m^2 radiation heat flux and the 100 kW flame. When the test was stopped the siding had cracked, but the combined siding/XPS construction remained stable, showing no signs that it would fail and cease protecting the home. Figure 18 shows the fiber cement/XPS sample at the conclusion of the combined radiation and convection test.

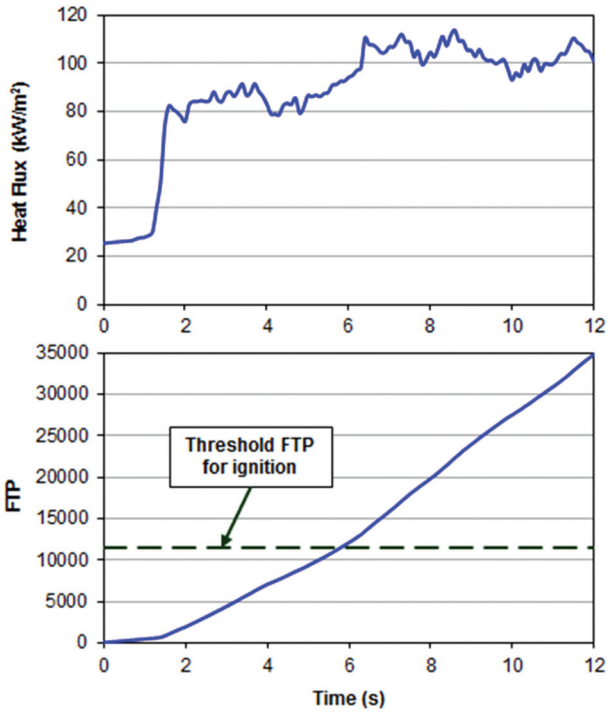

Figure 16 *Calculated incident heat flux (top) on the cedar sample for the combined radiant and convective exposure and the corresponding FTP values (bottom).*

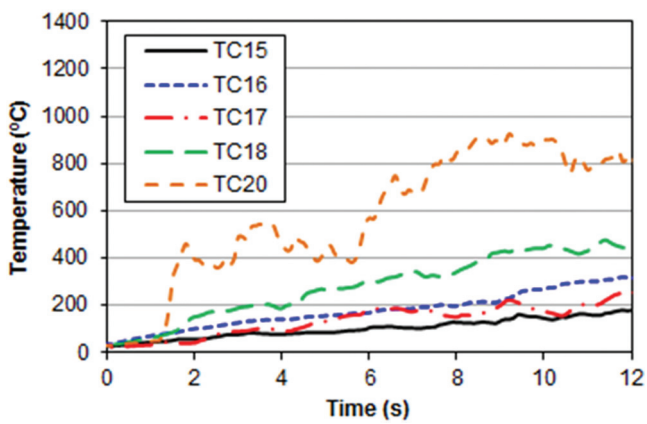

Figure 17 *Measured external cedar siding temperatures in response to combined radiant and convective heating.*

CONCLUSIONS AND FUTURE WORK

This paper describes a series of flammability tests of small-scale wall assemblies with different siding types that are commonly used in North America. These tests were designed to represent the radiant and convective heating of a building in the wildland-urban interface from common fire threats in the event of a wildfire. Data from these tests were

Figure 18 *Fiber cement board sample with XPS foam insulation at the end of the combined radiant and convective exposure test.*

utilized to validate and calibrate the calculation procedures within the structure ignition assessment model (SIAM), which is designed to allow homeowners to assess the level of ignition threat to their homes from their surroundings. The different siding types tested were cedar, vinyl, and fiber cement. The ignition threshold flux-time product embedded in the ignition model was verified by the radiant and convective tests of the wall samples with cedar siding. The convection calculation procedure was revised, with an updated constant heat transfer coefficient.

In addition to model validation, the tests provide important flammability data that can be utilized for future enhancements of the current model and also provide homeowners and community builders the knowledge to better design communities in the wildland-urban interface. Of the different sidings tested, the fiber cement siding proved to be non-combustible and the test data indicated that, for common fire threats, it could adequately protect the building exterior from failure by ignition.

The WildFIRE Wizard calculates the imposed heat flux on the structure and the response of the structure to heating. The former makes use of many estimated variables (e.g., the heat emitted from burning objects of various sizes, burning times, etc.), which can be estimated with greater confidence by performing laboratory tests. Ideally, a series of tests would be conducted with different burning objects that are typically present near a home (e.g., large shrub, shed, landscaping, etc.)

to precisely measure the time-dependent radiant heat flux. The Wizard also contains a module for calculating the risk to the home from airborne embers, mostly based on estimated probabilities. Tests exposing model homes to an ember attack would be ideal to better quantify these parameters.

ACKNOWLEDGMENTS

The authors would like to thank the Department of Homeland Security, Science and Technology Directorate, Infrastructure Protection & Disaster Management Division, for funding this research. This work was accomplished under Contract No. HSHQDC-08-X-00856 with the U.S. Department of Homeland Security. The contributions of Jack Cohen (Fire Sciences Laboratory, Missoula, MT), Jan Kosny (formerly with Oak Ridge National Laboratory, Oak Ridge, TN), Tim Smail (formerly with Savannah River National Laboratory, Aiken, SC), and Monica Philips (Savannah River National Laboratory, Aiken, SC) are gratefully acknowledged.

NOMENCLATURE

A	=	projected area, m^2
C	=	cooling rate, kW/m^2
C_p	=	heat capacity, $J/m^2 \cdot K$
c_p	=	specific heat, $J/kg \cdot K$
h	=	heat transfer coefficient, $kW/m^2 \cdot K$
Q	=	radiation exchange, W
Q''	=	heat flux, kW/m^2
Q_C''	=	critical radiant heat flux, kW/m^2
T	=	temperature, K
Δt	=	time step, s
v	=	view factor
ε	=	emissivity
σ	=	Stefan-Boltzmann constant, 5.67×10^{-8} $W/m^2 \cdot K^4$

Subscripts

f	=	flame
w	=	wall

REFERENCES

Albini, F. 1997. An overview of research on wildland fire. *Proc. Fifth International Symposium Fire Safety Sci.*, Melbourne, Australia, March 1997, pp. 59–74.

ASTM. 2011a. ASTM E 1269-11, *Standard Test Method for Determining Specific Heat Capacity by Differential Scanning Calorimetry.* West Conshohocken, PA, USA: ASTM International.

ASTM. 2011b. ASTM E 136-11, *Standard Test Method for Behavior of Materials in a Vertical Tube Furnace at 750°C.* West Conshohocken, PA, USA: ASTM International.

Cohen, J. 2004. Relating flame radiation to home ignition using modeling and experimental crown fires. *Can. J. For. Res.* 34:1616–26.

Hammer, R.B., S.I. Stewart, and V.C. Radeloff. 2009. Demographic trends, the wildland-urban interface, and wildfire management. *Soc. Nat. Resources* 22:777–82.

Incropera, F.P., and D.P. Dewitt. 1996. *Fundamentals of Heat and Mass Transfer*, 4th Ed. Wiley.

Lampin-Maillet, C., M. Jappiot, M. Long, D. Morge, and J.P. Ferrier. 2009. Characterization and mapping of dwelling types for forest fire prevention. *Comp., Env. Urban Systems* 33:224–32.

Manzello, S.L., T.G. Cleary, J.R. Shields, and J.C. Yang. 2006. Ignition of mulch and grasses by firebrands in wildland-urban interface fires. *Int. J. Wildland Fire* 15:427–31.

Manzello, S.L., A. Maranghides, and W.E. Mell. 2007. Firebrand generation from burning vegetation. *Int. J. Wildland Fire* 16:458–62.

Manzello, S.L., S-H. Park, and T.G. Cleary. 2009. Investigation on the ability of glowing firebrands deposited within crevices to ignite common building materials. *Fire Safety J.* 44:894–900.

Mell, W.E., M.A. Jenkins, J.S. Gould, and N.P. Cheney. 2007. A physics-based approach to modeling grassland fires. *Int. J. Wildland Fire* 16:1–22.

Mell, W.E., S.L. Manzello, A. Maranghides, D. Butry, and R.A. Rehm. 2010. The wildland-urban interface fire problem—Current approaches and research needs. *Int. J. Wildland Fire* 19:238–51.

Modest, M.F. 1993. *Radiative Heat Transfer.* McGraw-Hill.

MSC. 2008. *PATRAN*, Ver 2008 Rev. 1. Heat Transfer Software. MSC Software, Costa Mesa, CA.

NFPA. 2012. Quincy, MA: National Fire Protection Association. www.nfpa.org/research/fire-statistics/deadliest-and-large-loss-fires/largest-loss-wildland-fires

NIFC. 2012. Boise, ID: National Interagency Fire Center. www.nifc.gov/fireInfo/fireInfo_statistics.html

Papadopoulos, G.D., and F.-N. Pavlidou. 2011. A comparative review on wildfire simulations. *IEEE Systems J.* 5:233–43.

Reams, M.A., T.K. Haines, C.R. Renner, M.W. Wascom, and H. Kingre. 2005. Goals, obstacles and effective strategies of wildfire mitigation programs in the wildfire-urban interface. *Forest Policy Eco.* 7:818–26.

Rehm, R.G. 2008. The effects of winds from burning structures on ground-fire propagation at the wildland-urban interface. *Combustion Theory and Modeling* 12:477–96.

Theobald, D.M., and W.H. Romme. 2007. Expansion of the US Wildland-Urban Interface. *Landscape Urban Planning* 83:340–54.

Tieszen, S.R., T.J. O'Hern, R.W. Schefer, E.J. Weckman, and T.K. Blanchat. 2002. Experimental study of the flow field in and around a one meter diameter methane fire. *Combust. Flame* 129:378–91.

Xin, A., S.A. Filetyev, K. Biswas, J.P. Gore, R.G. Rehm, and H.R. Baum. 2008. Fire dynamics simulations of a one-meter diameter methane fire. *Combust. Flame* 153:499–509.